FLUKA Monte Carlo Simulations and Benchmark Measurements for the LHC Beam Loss Monitors

L. Sarchiapone, M. Brugger, B. Dehning, D. Kramer, M. Stockner, V. Vlachoudis
CERN, Geneva, Switzerland

Abstract

One of the crucial elements in terms of machine protection for CERN's Large Hadron Collider (LHC) is its beam loss monitoring (BLM) system. Online loss measurements must prevent the superconducting magnets from quenching and protect the machine components from damages due to unforeseen critical beam losses. In order to ensure the BLM's design quality, in the final design phase of the LHC detailed FLUKA Monte Carlo simulations were performed for the betatron collimation insertion. In addition, benchmark measurements were carried out with LHC type BLM's installed at the CERN-EU high-energy Reference Field facility (CERF). This paper presents results of FLUKA calculations performed for BLM's installed in the collimation region, compares the results of the CERF measurement with FLUKA simulations and evaluates related uncertainties. This, together with the fact that the CERF source spectra at the respective BLM locations are comparable with those at the LHC, allows assessing the sensitivity of the performed LHC design studies.

INTRODUCTION

The Large Hadron Collider (LHC) will collide proton beams at 14 TeV c.m. with unprecedented stored intensities. The LHC requires a stored energy of 360 MJ per beam and must be compared to a typical 10 mJ/cm^3 quench limit of the superconducting magnets. Therefore, a robust and highly efficient collimation system is required to withstand the high beam intensities and to absorb unavoidable beam losses. Two of the eight long straight sections of the LHC, see Figure 1, are therefore dedicated to beam collimation, point 3 (IR3) for momentum and point 7 (IR7) for betatron cleaning. At IR7 for nominal beam intensity at 7 TeV the specified peak loss rate corresponds to a total loss of 1% over 10 seconds only [1].
During LHC operation, only the accurate detection of the lost beam particles allows protecting the equipment by generating a beam dump trigger when the losses exceed certain thresholds. These thresholds depend on the momentum of the stored beam, the duration of the beam loss and on the location of the respective beam loss monitor. In addition to the quench prevention and damage protection, the loss detection allows the observation of local aperture restrictions, orbit distortions, beam oscillations and particle diffusion.

During the detector design detailed Monte Carlo simulations were performed in order to calculate the response of the BLM in a mixed radiation field [2], assess the expected particle loss spectra [3] and validate the necessary dynamic range of the detector [4].

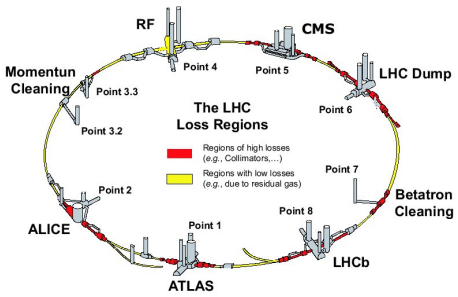

Figure 1: Distribution of high (red) and low (yellow) loss regions around the LHC. Especially the two beam cleaning insertions (Points 3 and 7) and the inner triplets will be regions of high continuous losses.

In order to evaluate the needed accuracy of the FLUKA [5, 6] simulations, performed for the LHC BLMs being installed close to the collimators in the cleaning insertions, this paper presents results of calculations performed for the collimation region with different levels of detail in the detector implementation and comparing them by studying particle energy spectra entering the sensitive volume of the detector as well as their respective energy deposition. The same approach has been followed for the CERF benchmark experiment quantifying, in addition, possible uncertainties due to applied conversion factors, beam shape as well as alignment and positioning.

LHC FLUKA MONTE CARLO SIMULATIONS

At the LHC four different families of beam loss monitors will be used, out of which the highest number of monitors will be installed around the super-conducting quadrupole magnets all around the accelerator ring (six per quadrupole). In the beam cleaning insertions one important set of detectors will be installed after each collimator in order to set the position of the collimator jaws, detect high losses and to continuously monitor their performance. The required extended dynamic range of 10^{13} is realized by installing two detectors with different sensitivities next to each other. The in this study considered standard monitors are ionization chambers with parallel aluminum electrode plates separated by 0.5 cm. The detectors are about 50 cm long with a diameter of 9 cm and a sensitive volume of 1.5 liter filled with Nitrogen at 100 mbar overpressure. For the

performed FLUKA studies two different geometrical implementations were studied, one only containing the outer container of the detector and a second modelling as detailed as possible the structure of the detector as shown in Figure 2.

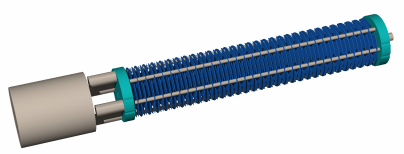

Figure 2: Inside structure of the ionization chamber as modeled in FLUKA.

IR7 Simulations results

A horizontal (ionization chamber) and a vertical (SEM) BLM are located downstream of each collimator, relatively close to the beam line. They will be used to measure the beam properties, the collimator alignment and trigger a beam dump in case of unacceptable high losses in the cleaning insertion. Any change in the jaw aperture will affect the distribution of interactions among the collimators and the propagation of the secondary cascade along IR7. This results in a change of the particle energy spectra seen by the BLM's and their recorded signal, thus allows measuring the respective loss rate by applying a correct calibration to each BLM. The latter is influenced by numerous parameters: the detector response, the loss distribution in the collimators, the cross-talk between the two circulating beams and their respective losses as well as by positioning and alignment uncertainties.

Therefore, FLUKA simulations were performed for a detailed analysis of the particle spectra entering the sensitive volume of each of the installed BLM detectors. For the first secondary collimator showing the highest losses Figure 3 shows particle energy spectra entering the active volume of the BLM, in the considered energy range of 100 keV to 100 GeV. Detailed BLM detector response functions were calculated for 0 and 90 degrees [2], however not for the exact model which will be used for the LHC but a former SPS type being different in its size and the layout of the internal electrodes. In addition, the detector response shows a significant dependency on the angular orientation of the detector with respect to the particle fluence, thus limits the usability of these response functions for the application in the collimation region where the spectra have their main origin in the collimators of the considered respective loss scenario as well as secondary interactions in additional upstream machine components.

Avoiding complications with the angular dependence of the BLM response and in order to profit from the new detailed geometrical implementation in FLUKA the energy deposition in the active volume is used as quantity calculated with FLUKA. The produced charge can then be deduced by dividing this value by the average energy neces-

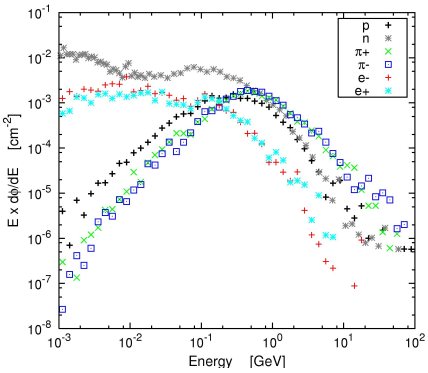

Figure 3: Spectra of particles in the IR7 BLM active volume.

Table 1: Main contributing particles for the respective radiation fields at IR7. All numbers are given in percent.

Target mat.	pos	orient.	p	π	e-	e+
IR7	TCSGA	ver	27.4	16.8	34.9	15.6

sary to produce an ion pair, the so-called *W*-factor. This conversion factor also accounts for other occurring processes like excitation, with the average energy lost in an energy deposition event usually being substantially greater than the ionisation energy. The *W*-factor is a function of the gas, the type of radiation and its energy. However, in the effective energy range and for the main contributing particle types the W-factor does not show a strong dependence, hence, can be approximated in most cases by a constant value for the respective gas type [7].

Including the detailed layout of the BLM detectors in the complete FLUKA simulation for the betatron cleaning insertion for each of the collimator positions and possible loss scenarios the total energy deposition and particle energy spectra were calculated in the BLMs. This allows to characterize the cross-talk between the BLM chambers as well as to define the signal thresholds for selected maximum loss rates (intensities). Selecting separately different particle types for the scoring in FLUKA shows the main contributing particles to the total signal as given in Table 1.

CERF EXPERIMENT

The experiment was performed at the CERN-EU high-energy Reference Field (CERF) facility [8]. At this facility a pulsed, 120 GeV/c mixed hadron beam (1/3 protons, 2/3 positively charged pions) from the Super Proton Synchrotron (SPS) accelerator is aimed at a 50 cm long copper or aluminum target creating a stray radiation field around the target that is similar to beam loss regions at high-energy accelerators (collimators, dumps, etc.). Figure 4 compares the FLUKA particle energy

spectra between CERF and the BLM locations in the LHC cleaning insertion, thus clearly motivating measurements of the LHC type BLM around the CERF target. All beam parameters, such as the number of particles per beam pulse (using a calibrated ionization chamber installed upstream of the target) and lateral profile of the beam (FWHM - horizontal: 2.3 cm, vertical: 2.1 cm) were recorded.

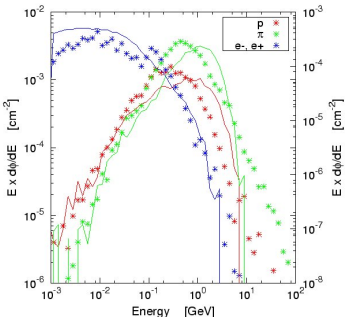

Figure 4: Spectra of particles in the IR7 (symbols) and CERF (lines) BLM active volume.

Two ionization chambers were placed in the target chamber at different locations: one of them is close to the beam impact point at 90° with respect to the beam direction, the other in forward direction downstream of the target at about 15° wrt the beam direction. Detailed FLUKA simulations were run to study the detector signal as a function of the location (15° or 90°), of the orientation (vertical or horizontal) and of the used beam target material aluminum or copper. For integral values the energy deposited by the cascade products in the nitrogen filling the space between electrodes was converted to charge using an average *W*-value of 35 eV/ion pair, [7].

FLUKA simulations

The influence to the integral signal changes with the target material and with detector position. As one can see from Table 2, with a copper target the main contribution comes from electrons. In the detector placed at 90° wrt the beam direction the contribution of protons is around 20%. At about 15°, downstream of the target, positrons, together with electrons, are dominant. With the aluminum target, the signal in the downstream detector is still given by electrons and positrons; upstream, however, protons have the main influence.

To better study the sensitive energy region of the detector, the detector response of the ionization chambers has been determined with Geant 4 simulations for different particle types [2]. The precalculated response functions were folded with the particle spectra in order to visualize the energy dependent detector signal. Figure 5 shows the spectrum, the response function and the folding of the two (in arbitrary units) for electrons at 90°, while Figure 6 shows the signal of the main contributing particles in a vertical

Table 2: Main contributing particles for the respective radiation fields at CERF. All numbers are given in percent.

Target mat.	pos	orient.	p	π	e-	e+
Cu	90°	ver	20.3	9.3	36.4	11.6
	15°	ver	11.6	10.9	47.7	20.8
	90°	hor	20.7	8.5	36.5	10.5
	15°	hor	11.9	11.6	48.0	19.6
Al	90°	ver	35.7	17.2	19.5	10.1
	15°	ver	8.2	9.3	49.9	26.2
	90°	hor	34.6	18.0	19.3	9.2
	15°	hor	8.9	9.6	49.4	25.1

detector at about 15° wrt the beam direction, showing a sensitive region between 10 MeV and 10 GeV.

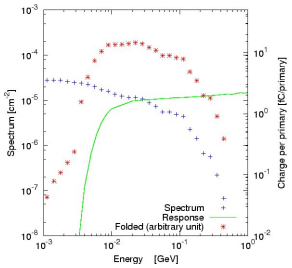

Figure 5: Spectrum, response function and expected signal for electrons at 15°.

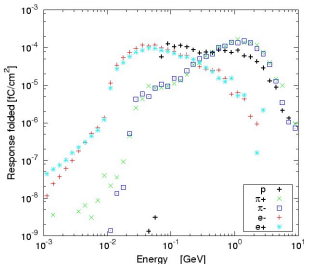

Figure 6: Signal of the main contributing particles in a vertical detector 15° wrt the beam direction.

To study the needed accuracy, Table 3 shows the influence of the level of detail in the description of the ionization chamber: in the not detailed description the energy is deposited in a simple cylinder containing the nitrogen gas, while in the complex one the energy is deposited in the actual space between the electrodes. As can be seen the difference between the two geometries is less than 8%.

Measurements

The comparison between simulated and measured signal is presented in Table 4. The agreement is good at 90° (position 3), where the observed differences stay within 12%,

Table 3: Simple and complex geometry results.

Target mat.	pos	orient.	Simple [aC/pot]	Complex [aC/pot]	ratio $\frac{simple}{complex}$
Cu	90°	ver	37.7	38.4	1.02
	15°	ver	72.8	67.2	0.92
Al	90°	ver	6.5	6.9	1.06
	15°	ver	51.5	47.5	0.92

Table 4: Comparison of FLUKA simulations results and measurements at the CERF target area.

Target mat.	pos	orient.	FLUKA sim. [aC/pot]	meas.	ratio $\frac{sim.}{meas.}$
Cu	90°	ver	37.7	28.8	1.31
	15°	ver	72.8	54.8	1.33
	90°	hor	36.3	34.3	1.06
	15°	hor	68.0	49.1	1.38
Al	90°	ver	6.5	6.2	1.05
	15°	ver	51.2	38.4	1.33
	90°	hor	6.2	7.0	0.88
	15°	hor	50.0	31.2	1.6

except for the Copper-vertical configuration. At the position 5 however the difference is in the order of 30% and even up to 60% for the aluminum target case.

Discussion of uncertainties

FLUKA simulations were performed accounting for all geometrical details, the correct beam alignment as well as the lateral beam shape. Statistical uncertainties are kept below five percent. The experimental setup includes positioning uncertainties in the order of one to two centimeter at most, thus leading to an expected signal change of not more than 5% [9]. Impinging beam intensities were monitored using an ionization chamber installed upstream of the target with a given calibration uncertainty of about 10%.

In order to account for the influence of the beam shape additional simulations were performed not including the measured beam distribution but assuming a pencil beam only. As shown in Table 5 for the copper target the influence is about 4% at 90° and 12% at 15° respectively.

The variation of the response in case of a possibly misaligned beam impact has been studied as well. Assuming a beam misalignment of only 1° leads already to a variation of the detector signal of 4% at position 3, and 20% at position 5. Table 6 shows results for angles between plus/minus two degrees as well as for the two different target materials.

In addition, the considered sensitive volume of the detector was considered as the active volume between the electrodes and taken from the detector specifications,

Table 5: Influence of the size of the impacting beam on the BLM signal. The influence is given as ratio between the gaussian and the pencil beam.

pos	Scenario	Influence [%]
90°	**gaussian/pencil**	1.04
15°	**gaussian/pencil**	1.12

Table 6: Influence of the beam impacting angle on the BLM signal. Values are given as ratio to the correctly aligned scenario.

Target mat.	pos	orient.	Impacting angle -2°	1°	2°
Cu	90°	ver	0.82	1.04	1.19
	15°	ver	0.65	1.18	1.56
	90°	hor	0.81	-	1.17
	15°	hor	0.58	-	1.67
Al	90°	ver	0.92	-	1.10
	15°	ver	0.71	-	1.38
	90°	hor	0.81	-	1.14
	15°	hor	0.70	-	1.37

where no detailed study was performed so far in order to estimate the respective uncertainties. Finally, as additional scaling factor also the uncertainty of the used *W*-factor has to be taken into account. The *W*-factor being a function of the gas, the type of radiation and its energy, does however not show a strong dependence in the given energy range and for the main contributing particle types. The given underlying uncertainties are estimated to be about 10%.

CONCLUSION

The LHC BLM system meets challenging requirements with the LHC tolerating less fractional beam losses than any other existing hadron machine. For the beam cleaning insertions BLMs will be used to set the position of the collimator jaws, detect high losses and trigger beam dumps as well as continuously monitor the collimator performance. Detailed FLUKA simulations studied for the entire set of BLMs installed in the betatron cleaning insertion the detector signal as a function of the particle losses as well as the cross-talk between losses occuring at different collimator locations. In addition, benchmark measurements at the CERF facility were performed, showing the comparable radiation fields between the LHC and the respective CERF measurement positions and allowing to successfully evaluate the simulations by studying the main contributing particles (protons, pions, electrons and positrons), their sensitive energy range (10 MeV to 10 GeV) as well as the influence of the considered detail of the simulated detec-

tor geometry. The comparison of simulations with measurements shows an overall overestimation of the simulation between 10 and 30% with more scattered values for the aluminum target. Former studies (using a similar detector type) showed a better match, thus lead to the discussion of underlying uncertainties considering the statistical uncertainties of the simulation (5%), the positioning (5%), the beam profile (4-12%), the beam intensity (10%), the alignment of the beam (8-30%) as well as the used *W*-factor (10%). The pessimistic overall uncertainty can thus be estimated to be rather high and mainly dominated by the beam alignment. The high sensitivity of the detector signal to only small changes in the source term suggests that for the use at the LHC further careful simulations and measurements are necessary in order to precisely define final detector calibration factors and thresholds.

ACKNOWLEDGEMENTS

We would like to thank the SC/RP group for their help setting-up and providing the CERF facility, Christian Theis and Helmut Vincke for many stimulating discussions, as well as Paola Sala for providing the detailed FLUKA input of the BLM chamber.

REFERENCES

[1] CERN, "The LHC Design Report, Vol. I: The LHC Main Ring", Technical Report CERN-2004-003 (2003).

[2] M. Stockner et al., "Measurements and Simulations of Ionization Chamber Signals in Mixed Radiation Fields for the LHC BLM System", Proceedings of IEEE 2006, San Diego/CA-USA (2006).

[3] M. Magistris, M. Santana-Leitner, V. Vlachoudis, A. Ferrari, "FLUKA simulations for the optimization of the Beam Loss Monitors", CERN AB Internal Note (2006).

[4] E. B. Holzer et al., "Beam Loss Monitoring System for the LHC", CERN AB Internal Note, CERN-AB-2006-009 (2006).

[5] A. Fassó, A. Ferrari, J. Ranft, and P.R. Sala, "FLUKA: a multi-particle transport code", CERN-2005-10 (2005), INFN/TC_05/11, SLAC-R-773.

[6] A. Fassó, A. Ferrari, J. Ranft, P.R. Sala, "The physics models of FLUKA: status and recent developments", Computing in High Energy and Nuclear Physics 2003 Conference (CHEP2003), La Jolla, CA, USA, March 24-28, 2003, (paper MOMT005), eConf C0303241 (2003), arXiv: hep-ph/0306267.

[7] 7^{th} International Commission on Radiation Units and Measurements, Average Energy Required To Produce An Ion Pair, ICRU Report 31, Washington D.C. (1979)

[8] Mitaroff, A. and Silari, M. The CERN-EU high-energy reference field (CERF) facility for dosimetry at commercial flight altitudes and in space. Radiat. Prot. Dosim. 102, 7-22 (2002).

[9] H. Vincke et al., Measurements and Simulations of the PMI Chamber Response to the Radiation Field inside the CERF Target Area, CERN SC Internal Note, CERN-SC-2004-025-RP-TN (2004).